Ying GAO[1], Baifen LIU[2]

East China Jiaotong University (1),(2)

Active-Disturbance Rejection Control for a Direct-Drive Valve based on a linear motor

Abstract. A novel control scheme for a linear motor drive is proposed in this paper. Voice coil motor VCM, as one of the linear motors, which is widely used in the field of direct drive servo valve (DDV) with superior performance, has high accuracy and fast transient response. However, there are such uncertainties as unpredictable hydraulic resistance and estimated errors of the VCM model in this system, which may influence the accuracy and the rapid response of the control. In this paper, ADRC is applied to the system, which has strong robustness. Simultaneously, a novel hardware structure of motor control system based on field programmable gate array (FPGA) and digital signal processor (DSP) is implemented to realize the proposed algorithm. Both simulation and experimental results verify that the scheme proposed can attenuate the influences by the uncertainties of the model sharply. Also, the static and dynamic performances of the control system have been improved greatly with strong robustness to disturbances. Furthermore, the rapidness of the system has been improved greatly.

*Streszczenie. W artykule przedstawiono system sterowania silnikiem liniowym ADRC bazujący na układach FPGA i wykorzystujący procesor sygnałowy. Silnik typu VCM (voice coil motor) jest używany do servo zaworu. (**Aktywne sterowanie z usuwaniem zakłóceń do napędu zaworu z silnikiem liniowym**)*

Keywords: direct-drive valve (DDV), active-disturbance rejection control (ADRC), digital signal processor (DSP), field programmable gate array (FPGA).
Słowa kluczowe: zawór DDV, FPGA, DSP.

Introduction

The direct drive servo valve (DDV), which has good features as high-frequency response, large flow high-power density and excellent anti-contamination characteristics, is extensively utilized in the research and application fields of modern aviation and aerospace, military, chemical industry, industrial automation, etc [1-3]. Traditionally, a DDV is actualized by rotating motors with complex mechanical transmission mechanism, which causes complexity in mechanical structure, bulkiness in volume, slow responses, low positioning precision, and dynamic performance. As a result, great attention has been paid to the voice coil motor (VCM) [4-7], one of the linear motors, which greatly simplifies the mechanical structure and improves the precision and response speed. A voice coil motor has the advantages of small volume, low cost, simple structure, high flux density, reliability, and easy control [8, 9].

n many industrial drives, advanced digital control strategies for the control of VCM drives with a conventional position controller. Proportional-integral-deriative (PID) controller, has gained the widest acceptance in high-performance ac servo systems [10, 11]. Generally, the position controller of the VCM is requested to have a rapid and accurate response for the reference, regardless of whether a load disturbance is imposed and the plant's parameters vary. However, the conventional PI control scheme has a steady-state error and a long recovery time when a load disturbance is imposed [12, 13]. The conventional PI control scheme cannot obtain good position response. Several methods have been reported to minimize the consequences of parameter sensitivity in controlled drives.

There exist some uncertainties for VCM, including model estimating errors and unpredictable hydraulic disturbance. In this paper, active disturbance rejection control (ADRC) and a neural network identifier (NNI) are introduced into system to realize the robust control of the DDV.

Modeling of direct drive servo valve system with voice coil motor

As is shown in Fig.1, the whole system consists of a voice coil motor, a hydraulic valve, an intelligent motor controller and a position sensor. The valve has outstanding features of high response due to the compact and powerful linear motor，VCM. It directly drives the spool and gives the feedback of the spool position. The orifice area is varying on account of the relative motion between the spool and the valve housing. Regardless of the leakage of the valve, the rate of flow which crosses the valve is

$$(1) \qquad Q_v = C_d \omega x_v \sqrt{\frac{2\Delta p}{\rho}} = K_Q x_v$$

where, Q_v represents the flow of the valve, C_d is the coefficient of the flow, ω is the moment inertia, x_v is the displacement of the spool, Δp is the, ρ is the oil fluid density, K_Q is the coefficient of the flow. It can be seen that the flow of the valve is determined by the position of the spool.
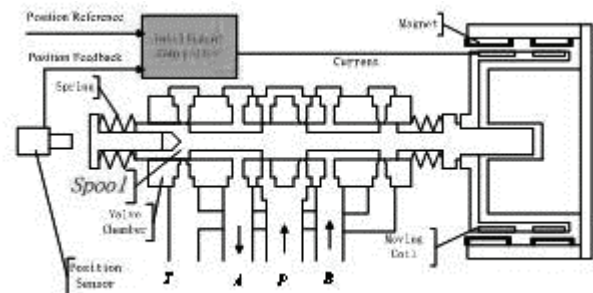

Fig.1. The structure of the DDV

Assuming that the performance of power devices of the inverter ids ideal, and ignoring armature reaction, slot effect, and iron losses, the voltage equation for a VCM can be described as

$$(2) \qquad u_a = R_a i_a + L_a \frac{di_a}{dt} + e_a$$

where u_a represents the terminal voltage with respect to power ground, i_a is the current of the voice coil, e_a is the back-EMF of the voice coil, R_a and L_a are resistance and inductance of the winding of the VCM, respectively.

When the fluid flows through the valve port, the flow direction and velocity changes in the size of the change will

result in the fluid momentum. The resulting flow of additional forces on the spool, the role of this force is called the liquid in the spool on the power. According to the nature of fluid power, hydraulic power can be divided into steady and transient hydraulic force.

(3)
$$F_s = -2C_d C_V \omega x_v \Delta p \cos \theta$$

(4)
$$F_t = (L_1 - L_2) C_V \omega \sqrt{\rho \Delta p} \frac{dx_v}{dt}$$

where F_s and F_t represent the steady hydraulic force and the transient hydraulic force, respectively. X_v is the displacement of the spool. On account of the possibility that there are some parameters in equation (5) and (6) are shifting when the valve starts to work, some unpredictable influences may happen to the control system. So it is needed to seek for the scheme to attenuate the influences of the forces. The whole control modeling is shown in Fig.2. And the proposed scheme is implemented in the position-loop controller.
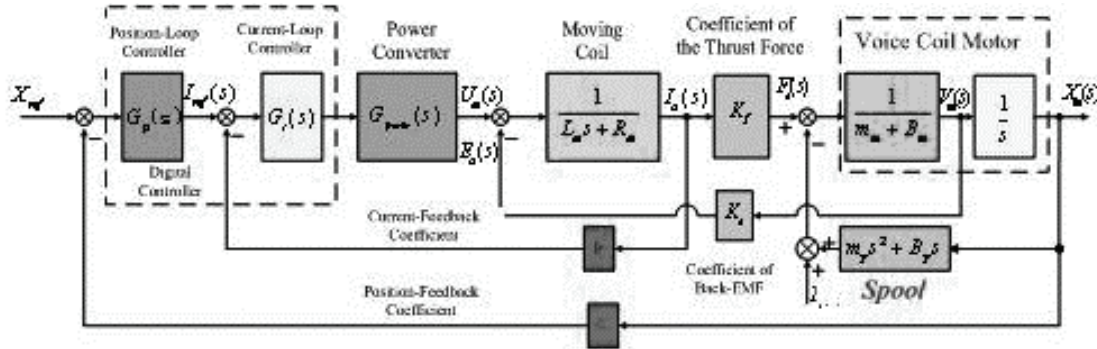

Fig.2. Schematic of system modelling diagram

The proposed control scheme
As discussed in section 2, there are both a stable flow force and a transient flow force in DDV. There is the need to seek for a scheme to attenuate the effects of the forces. Compared to other schemes, ADRC has good performances with less computational burden and excellent robustness.

Many plant models can be simplified as follows

(5)
$$x^{(n)} = f(x, \dot{x}, \cdots, x^{(n-1)}, t) + w(t) + u$$

where, w is an external disturbance variable, u is a control variable and $f(x, \dot{x}, \cdots, x^{(n-1)}, t)$ is an uncertain plant. For the two-order plant, its standard ADRC controller structure.

An ADRC controller consists of three main parts:tracking differentiator ,nonlinear feedback and an extended-state observer.

The tracking differentiator arrangement is as follows

(6)
$$\begin{cases} e = v_1 - v_0 \\ fh = fhan(e, v_2, r_0, h) \\ v_1 = v_1 + h \cdot v_2 \\ v_2 = v_2 + h \cdot fh \end{cases}$$

Where V_1 is the control objective, V_2 is the track signal of V_3 and $fhan()$ is a time optimal integrated function, whose detailed expression is described as (7). In general, in the ADRC framework, a tracking differentiator is used to construct a reference position observer in terms of the reference velocity.

(7)
$$\begin{cases} d = r \cdot h, d_0 = r \cdot d, y = x_1 + h \cdot x_2 \\ a_0 = \sqrt{d^2 + 8r \cdot |y|} \\ a = \begin{cases} x_2 + \frac{(a_0 - d)}{2} sign(y), |y| > d_0 \\ x_2 + \frac{y}{h}, |y| \le d_0 \end{cases} \\ fhan = -\begin{cases} r \cdot sign(a), |a| > d \\ r \frac{a}{d}, |a| \le d \end{cases} \end{cases}$$

Generally, higher bandwidths of the observer and controller result in better performance of tracking and disturbance rejection. However, the higher the bandwiths are, the larger the ripple threshold for the control signal is . This is mainly due to the presence of sensor noise. High bandwidths cause much sensor noise to pass on to the control actuator. Therefore, the tuning parameters should reach a tradeoff between the bandwidths and the control signal ripple that does not significantly impair the actuator activity. So an extended-observer is shown as below

(8)
$$\begin{cases} d = r \cdot h, d_0 = r \cdot d, y = x_1 + h \cdot x_2 \\ a_0 = \sqrt{d^2 + 8r \cdot |y|} \\ a = \begin{cases} x_2 + \frac{(a_0 - d)}{2} sign(y), |y| > d_0 \\ x_2 + \frac{y}{h}, |y| \le d_0 \end{cases} \\ fhan = -\begin{cases} r \cdot sign(a), |a| > d \\ r \frac{a}{d}, |a| \le d \end{cases} \end{cases}$$

where h is the sampling period.

(9)
$$\begin{cases} e_1 = v_1 - z_1, e_2 = v_2 - z_2, \\ u_0 = \beta_1 \cdot fal(e_1, \alpha_1, \delta) + \beta_2 \cdot fal(e_2, \alpha_2, \delta) \end{cases}$$

We propose the following nonlinear function

(10)
$$\begin{cases} e_1 = v_1 - z_1, e_2 = v_2 - z_2, \\ u_0 = \beta_1 \cdot fal(e_1, \alpha_1, \delta) + \beta_2 \cdot fal(e_2, \alpha_2, \delta) \end{cases}$$

Simulation and experimental results

To verify the correctness and feasibility of the proposed scheme for the VCM, a complete simulation system was built. The simulation results are compared with those of the PID controller.

The specifications of the VCM are shown in Table 1.

Table 1. Specifications of the VCM

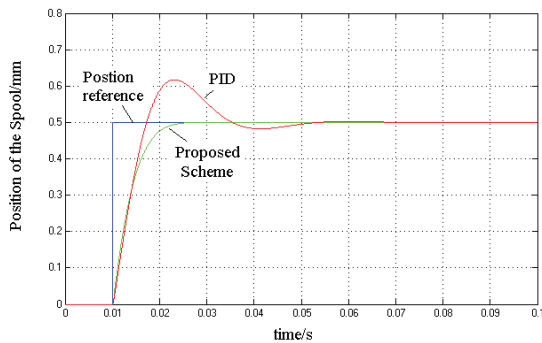| Parameters	Quantity	Parameters	Quantity
Voltage (V)	48	Controlling Cycle of the Current Loop (us)	25
Resistor (Ω)	5	Controlling Cycle of the Position Loop(us)	100
Inductance (mH)	2	Rated Thrust Force of the Motor(N)	60
Maximum Current (A)	6	Quality of the Moving Coil (Kg)	0.1
Coefficient of the Force(N/A)	20		

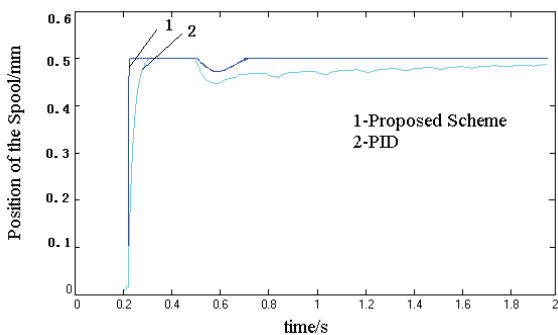Fig.3. Comparison of tracking of different algorithms

Fig.4. Robustness of different algorithms to disturbance

It can be clearly seen from the Fig.3 that the rising time is longer while using traditional PID. There are also system overshoot and oscillations and the control system can not meet the demands. It illustrates that when the motor is controlled by the proposed scheme, there is no overshoot and rising time is also very short (4ms).

Fig.4 shows the desired and actual trajectories of the spool displacement where a hydraulic disturbance (30N) is added to the controlling system at the time 0.6s. It validates that the scheme proposed can attenuate the influences by the uncertainties of the model sharply.

The whole system is implemented by the TMS320-VC33 DSP and EP2C35S208C8N FPGA. The configuration of the experimental system is shown in Fig.5.
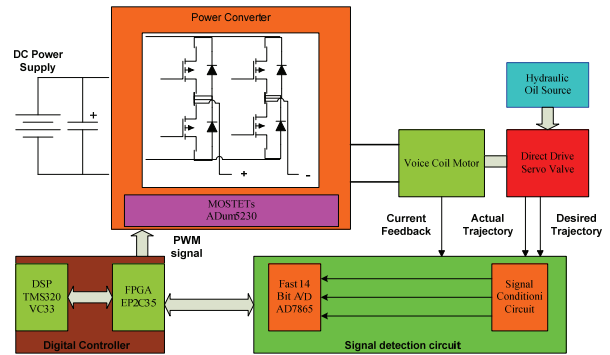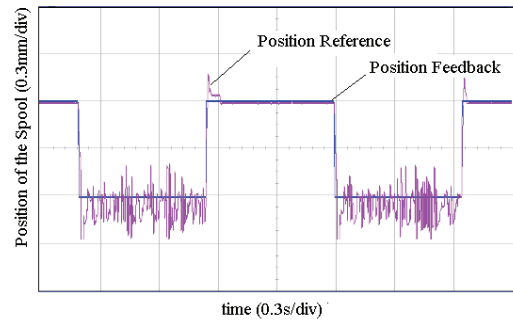

Fig 5. Schematic of system implementation

Fig.6. Experimental waveforms in the track of 1Hz square wave when the motor is controlled by PID
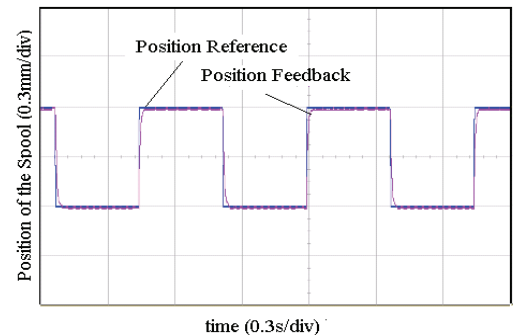

Fig.7. Experimental waveforms in the track of 1Hz square wave when the motor is controlled by proposed algorithm

A hypothetical microprocessor system in which the proposed algorithm can be implemented is proposed in the following. Hardware architecture of this controller is based on TMS320VC33 DSP and CYCLONE II FPGA. TMS320VC33 is a high performance DSP with 32-bit floating-point, 17-ns instruction cycle time and 120 million floating-point operations per second. TMS320VC33 supports programming with both C language and assembly language. And it can carry out complex calculation easily. CYCLONEII FPGA is based on a 1.2V, 90-nm SRAM process with densities over 64K logic elements, up to 1.1Mbits of embedded RAM and embedded 18 multipliers. With this features, it supports high performance DSP applications.

The position signal of the spool is obtained by a sensor. Position signal is inputted into the FPGA. The control system is composed of two loops: position and current loops. The position loop is the outer loop of the control system, and the current loop serve as the inner loop of the control system. The proposed control scheme will be implemented on the position loop. The position commands

sent from Upper Computer are inputted into the FPGA through the Serial port. The output of the position loop is the desired signal of the current loop, and the current sampling signal inputted into the FPGA through the A/D port. Then, 40 KHz pulse width modulation (PWM) waveform whose duty is calculated by the DSP is generated by FPGA. After the Optical Coupling Isolation and Driving Amplification of driving circuit, the PWM-inverter-modulating signals will control MOSFETs in the full-bridge circuit to be turned on and off, and the control of position can be actualized. And the overcurrent protection is also implemented in FPGA. Some basic experiments have been done according to Fig.6-Fig.7.

Fig.6 and Fig.7 show the significant difference of the two results which suggest that the controller with the proposed scheme can reject such fluid disturbances well and maintain good tracking performances both in reference of 1Hz square wave and sine wave.

The aforementioned simulation and experimental results demonstrate the controller's ability to estimate and compensate for uncertainties and variant cutting disturbances caused by the fluid force. The static and dynamic performances of VCM are greatly improved after the algorithm is applied.

Conclusions

This paper has proposed a dynamic model of VCM and has put forward a novel control scheme according to this model. In the algorithm, ADRC is applied to the system, which has strong robustness. Simultaneously, a novel hardware structure of motor control system based on field programmable gate array (FPGA) and digital signal processor (DSP) is implemented to realize the proposed algorithm. Simulation and experimental results validate the scheme proposed can attenuate the influences by the uncertainties of the model sharply. Also, the static and dynamic performances of the control system have been improved greatly with strong robustness to disturbances.

REFERENCES
[1] Jea-Sen Lin and Chern-Lin Chen, "Buck/boost servo amplifier for direct-drive-valve actuation," IEEE Transactions on Aerospace and Electronic Systems, vol.31, issue 3, pp.960-967, July 1995.
[2] Jian-Feng Tao, Lin-Shan Jin, Lei Xu and Cheng-Liang Liu, "Load control of electrically controlled hydraulic pump's flow/pressure characteristics testing with direct drive servo-proportional valve," 2010 IEEE/ASME International Conference on Advanced Intelligent Mechatronics (AIM), pp.1374-1378, July 2010.
[3] Miao-Lei Zhou, Zhi-Gang Yang, Wei Gao, Yan-Tao Tian, Chuan-Liang and Shen Peng-Li, "Fuzzy Control of a new type of piezoelectric direct erive electro-hydraulic servo valve," vol 2, pp.819-823, August 2005.
[4] Myeong-Gyu Song, Jung-Hyun Woo, No-Cheol Park, Jeonghoon Yoo, Young-Pil Park and Kyoung-Su Park, "Design of the rotary VCM actuator for small form factor optical disk drive," Microsystem Technologies, vol.16, no.1-2, pp.205-212, 2010.
[5] Landolsi Taha, Dhaouadi Rached, Aldabbas Oubadah, "Beam-stabilized optical switch using a voice-coil motor actuator," Journal of the Franklin Instirute, vol.348, no.1, pp.1-11, January 2011.
[6] Jong-kyu Jung, Woo-seub Youm, Kyi-hwan Park, "Vibration reduction control of a voice coil motor (VCM) nano scanner," International Journal of Precision Engineering and Manufacturing, vol.10, no.3, pp.167-170, 2009.
[7] Chien-Sheng Liu, Psang-Dain Lin, Po-Heng Lin, Shun-Sheng Ke, Yu-Hsiu Chang and Ji-Bin Horng, "Desing and characterization of miniature auto-focusing voice coil motor actuator for cell phone camera applications", IEEE Transactions on Magnetics, vol.45, no.1, pp.155-159, June 2009.
[8] Shir-Kuan Lin, Chao-Min Wang and Shyh-Jier Wang, "Design and implementation of anti hand shaking position control for a voice coil motor," Journal of Applied Physics, vol.103, no.7, pp.07F128, 2008.
[9] Hsing-Cheng Yu, T.S. Liu, "Adaptive model-following control for slim voice coil motor type optical image stabilization actuator," Journal of Applied Physics, vol.103, no.7, pp.07F114, 2008.
[10] Welander Peter, "Understanding derivative in PID control," Control Engineering, vol.57, no.2, pp.24-27.
[11] Densisenko V.V., "Modifications of PID regulators," Automation and Remote Control, vol.71, no.7, pp.1465-1475, 2010.
[12] Farag A. and Werner H. "Structure selection and tuning of multi-variable PID controllers for an industrial benchmark problem," Control Theory and Applications, vol.153, no.3 pp.262-267, 2006.
[13] Visioli A. "Modified anti-windup scheme for PID controllers," Control Theory and Applications, vol.150, no.1, pp.49-54, 2003.

Authors: *Associate professor. Ying Gao, School of basic sciences, East China Jiao tong University, Shuanggang Road, Nanchang, JiangXi Province. E-mail: chair0088@yahoo.com.cn.; Prof. Baifen Liu, School of electronic and electrical engineering, East China Jiao tong University, Shuanggang Road, Nanchang, JiangXi Province. E-mail: bfliu@yahoo.com.cn.*